Title

Repair of injured urethras with silk fibroin scaffolds in a rabbit model of onlay urethroplasty

Authors

Algarrahi, Khalid
Affas, Saif
Sack, Bryan S
et al.

Publication Date

2018-09-01

DOI

10.1016/j.jss.2018.04.006

Peer reviewed

HHS Public Access

Author manuscript

J Surg Res. Author manuscript; available in PMC 2019 September 01.

Published in final edited form as:

J Surg Res. 2018 September ; 229: 192–199. doi:10.1016/j.jss.2018.04.006.

Repair of Injured Urethras with Silk Fibroin Scaffolds in a Rabbit Model of Onlay Urethroplasty

Khalid Algarrahi[a,b], **Saif Affas**[a,b], **Bryan S. Sack**[a,b], **Xuehui Yang**[a], **Kyle Costa**[a], **Catherine Seager**[a,b], **Carlos R. Estrada Jr.**[a,b], and **Joshua R. Mauney**[a,b,c]

[a]Urological Diseases Research Center, Boston Children's Hospital, Boston, MA 02115, USA

[b]Department of Surgery, Harvard Medical School, Boston, MA 02115, USA

Abstract

Background—Preclinical validation of scaffold-based technologies in animal models of urethral disease is desired to assess wound healing efficacy in scenarios which mimic the target patient population. This study investigates the feasibility of bi-layer silk fibroin (BLSF) scaffolds for the repair of previously damaged urethras in a rabbit model of onlay urethroplasty.

Materials and methods—A focal, partial thickness urethral injury was created in adult male rabbits (N=12) via electrocoagulation and then onlay urethroplasty with 50 mm^2 BLSF grafts was carried out 2 weeks post-injury. Animals were randomly divided into three experimental groups and harvested at 2 weeks post-electrocoagulation (N=3), 1 (N=3) or 3 (N=6) months following scaffold implantation. Outcome analyses were performed pre-operatively and at 2 weeks post-injury in all groups as well as at 1 or 3 months after scaffold grafting and included urethroscopy, retrograde urethrography (RUG), histological and immunohistochemical (IHC) analyses.

Results—At 2 weeks post-electrocoagulation, urethroscopic and RUG evaluations confirmed urethral stricture formation in 92% (N=11/12) of rabbits. Gross tissue assessments at 1 (N=3) and 3 (N=6) months following onlay urethroplasty revealed host tissue ingrowth covering the entire implant site. At 3 months post-op, RUG analyses of repaired urethral segments demonstrated a 39% reduction in urethral stenosis detected following electrocoagulation injury. Histological and IHC analyses revealed the formation of innervated, vascularized neotissues with α-smooth muscle actin+ and SM22α+ smooth muscle bundles and pan-cytokeratin+ epithelium at graft sites.

Conclusions—These results demonstrate the feasibility of BLSF matrices to support the repair of previously damaged urethral tissues.

[c]Corresponding author: Joshua R. Mauney, Ph.D., Boston Children's Hospital, Department of Urology, John F. Enders Research Laboratories, 300 Longwood Ave., Rm. 1009, Boston, MA 02115, USA; Phone: 617-919-2521; Fax: 617-730-0248; joshua.mauney@childrens.harvard.edu.

Disclosures: The authors have no financial disclosures or conflict of interests to declare.

Author contributions: K.A., B.S., J.R.M., and C.R.E. conceived and designed the experiments and analyzed data. K.A., S.A., C.S., X.Y., K.C., J.R.M. performed experiments, processed and analyzed data. All authors edited the paper. J.R.M. wrote the paper and supervised all aspects of the study.

Keywords

urethra; biomaterial; tissue engineering; stricture

Introduction

Pediatric and adult disorders of the urethra including hypospadias, trauma, and stricture disease represent significant health care burdens which require surgical intervention to replace developmentally absent or damaged tissue in order to preserve urinary tract function.[1,2] Autologous tissue grafts derived from extragenital skin flaps or buccal mucosa are primarily utilized to restore urethral continuity in cases where end-to-end anastomosis is not feasible.[3,4] However, these approaches have been associated with adverse side effects including stricture recurrence, diverticulae and fistula formation with total complication rates of 5–54%.[5–8] Moreover, the harvesting of autologous tissues requires secondary surgical procedures, is associated with morbidity at the donor site, and donor tissue volume is often limited for reconstructive procedures.[9] These issues highlight the critical need for the development of alternative strategies for urethral repair.

Bi-layer silk fibroin (BLSF) matrices represent emerging, biodegradable platforms for urethroplasty. The multi-functional graft configuration facilitates initial defect consolidation and maintenance of urethral integrity via a fluid-tight film layer, whereas host tissue integration is promoted via a porous foam compartment.[10,11] A previous study from our laboratory has demonstrated the feasibility of these grafts for onlay urethroplasty in a nondiseased, rabbit model of acute trauma wherein urethral reconstruction was performed immediately following creation of a full thickness defect.[11] In this setting, BLSF scaffolds promoted constructive remodeling of urethral defects with neotissues capable of supporting micturition and normal urethral continuity. Parallel evaluations with conventional small intestinal submucosa (SIS) scaffolds revealed BLSF matrices displayed superior biocompatibility with significantly less chronic inflammatory reactions at implantation sites.

Validation of biomaterial technologies in diseased animal models which mimic underlying patient pathology is necessary to accurately evaluate graft potential prior to clinical translation. Alterations in the regenerative capacity of host tissues can occur as a function of disease or past injury and can ultimately influence implant functional performance.[12–14] In particular, onlay urethroplasty of damaged rabbit urethras with SIS grafts showed delayed epithelialization and abnormal distribution of smooth muscle tissue in comparison to the results achieved in healthy cohorts.[13] In addition, patients who have undergone two or more failed urethroplasties and have comorbidities associated with urethral stricture disease present with an increased risk of repeat urethroplasty failure.[15] Therefore, the purpose of this study was to evaluate the ability of BLSF scaffolds to mediate tissue regeneration in urethras previously subjected to surgical injury in a rabbit model of onlay urethroplasty.

Materials and Methods

Biomaterials

BLSF grafts were fabricated from aqueous silk fibroin solutions derived from *Bombyx mori* silkworm cocoons using a solvent-casting/salt-leaching protocol in combination with silk fibroin film casting as previously described.[10] The structural and tensile properties of the scaffold have been reported in published reports.[10] Biomaterials were autoclaved sterilized prior to surgical manipulations.

Surgical Procedures

All animal studies followed guidelines prescribed by the National Institutes of Health's Guidelines for the Care and Use of Laboratory Animals and were approved by the Boston Children's Hospital Animal Care and Use Committee prior to experimentation and performed under protocol 15-06-2966R.

A focal, partial thickness urethral defect was induced in adult male New Zealand white rabbits (N=12, ~3–3.5 kg, Millbrook Breeding Labs, Amherst MA) using a previously described electrocoagulation injury model.[16] Adult male rabbits were utilized in these studies since their anatomy permits transurethral instrumentation with a standard urethroscope.[17] In addition, the urethra of male rabbits histologically resembles the human male with a stratified epithelium supported by vascularized spongious tissue.[17] Female rabbits were excluded from these investigations due to their short urethral length for reconstructive procedures. Under isoflurane inhalation and following intramuscular injection of 0.04 mg/kg glycopyrrolate, animals were placed in the supine position and genitalia were scrubbed with a povidine-iodine solution. Rabbits were kept under mechanical ventilation for the duration of the operative procedures. Animals were first subjected to imaging evaluations (retrograde urethrography and urethroscopy) to confirm normal anatomy. Next, a 2–3 mm wide electrocoagulation injury (1 cm in length) in the anterior urethral spongiosum was performed from the 3–9 o'clock position ~2 cm proximal to the external meatus using an electrosurgical loop from a pediatric resectoscope under direct visualization with a urethroscope. Following urethral injury, free urine drainage via catheterization was maintained for 1 week post-op with an 8 French Zaontz urethral stent, afterwards animals were allowed to voluntary void. Two weeks post-injury, imaging evaluations were carried out and rabbits were either euthanized for baseline histological and immunohistochemical (IHC) analyses (N=3) or subjected to BLSF scaffold implantation (N=9). A nonsurgical control (NSC) group of 3 rabbits was evaluated in parallel for all outcome analyses.

Ventral onlay urethroplasty with BLSF scaffolds was performed as previously described.[11] Following urethral catheterization, the penile urethra was sterilely exposed through a ventral midline penile skin incision and mobilized from the underlying corpora cavernosa under isoflurane anesthesia. A 5 × 10 mm (length × width) elliptical defect was created at the original injury site via excision of ventral urethral tissue with the penis on partial stretch. A BLSF graft of equal size was anastomosed to the defect using interrupted 6-0 polyglactin sutures. Nonabsorbable 6-0 polypropylene sutures were positioned at the proximal, distal, and lateral boundaries of the implant perimeter for identification of graft borders. Running

sutures were utilized to close skin incisions. Rabbits were administered prophylactic antibiotics (5 mg/kg/d Baytril®) for 3 days post-op and catheterization with an 8 French Zaontz urethral stent was maintained for a 7 day period after which voluntary voiding was permitted. Animals were harvested at 1 (N=3) or 3 (N=6) months post-repair for study endpoint evaluations.

Retrograde urethrography (RUG) and urethroscopy

RUG and urethroscopic analyses were carried out in nonsurgical controls and experimental animals prior to injury, 2 weeks post-injury, as well as 1 and 3 months following scaffold implantation to assess organ continuity and the presence of urethral abnormalities. For RUG evaluations, a 14G angiocatheter connected to an IV extension was inserted into the urethral meatus under isoflurane anesthesia and 170 mg/ml ioversol (Optiray™320, Liebel-Flarsheim Company LLC, Cincinnati, OH) contrast was infused in a retrograde fashion into the urinary tract while X-rays were acquired in supine and lateral positions. The degree of urethral stenosis in experimental groups was determined by calculating the percentage of the luminal urethral diameter at injured/repaired positions relative to a distal non-injured internal control region located ~1 cm from the urethral meatus. In addition, pre-operative assessments were performed similarly on corresponding urethra locations and served as baseline controls. The length of urethra strictures was also quantified from RUG photomicrographs. Urethroscopic surveillance was carried out by advancing a urethroscope into the urethral meatus to the injured/repaired site where the entire mucosal circumference was inspected. Images were acquired using an Olympus® video processor (Olympus® CV-100 video processor, Tokyo, Japan).

Histological, IHC, and histomorphometric analyses

Following animal harvest, penile tissue segments from NSC as well as experimental groups containing the original electrocoagulation injury region or implant site were excised for routine histological processing. Specimens were then fixed in 10% neutral-buffered formalin, dehydrated in graded alcohols, and embedded in paraffin. Sections (5 μm) were cut and stained with Masson's trichrome (MTS) using standard methods. Parallel sections were subjected to IHC analyses utilizing primary antibodies to select antigens including α-smooth muscle actin (SMA) [Sigma-Aldrich, St. Louis, MO, 1:200 dilution], SM22α [Abcam, Cambridge, MA, 1:200 dilution], pan-cytokeratin (CK) [Dako, Carpinteria, CA, 1:150 dilution], and neurofilament 200 (NF200) (Sigma-Aldrich, 1:250 dilution]. Samples were then incubated with species-matched, Cy3-conjugated secondary antibodies (Millipore, Billerica, MA) while 4′, 6-diamidino-2-phenyllindole (DAPI) was used as a nuclear counterstain. An Axioplan-2 microscope (Carl Zeiss MicroImaging, Thornwood, NY) was employed for sample visualization and representative fields were acquired with Axiovision software (version 4.8). Histomorphometric evaluations (N=3–6 rabbits per group) were performed on at least 6 independent microscopic fields equally dispersed along the entire graft or injury site as well as NSC using published procedures.[11] Image thresholding and area measurements were executed with ImageJ software (version 1.47). For α-SMA and pan-CK assessments, the percentage of tissue area stained per total field area examined was calculated. For NF200 evaluations, the total number of NF200+ nerve trunks per total field

area analyzed was determined. For all markers, relative immunoreactivity per field was computed by normalizing levels in experimental groups to NSC values.

Statistical Evaluations

Quantitative measurements for the degree of urethral stenosis and histomorphometric parameters were as follows: multi-group comparisons were performed using a one-way analysis of variance (ANOVA) test. In two group comparisons, a two-tailed Students t-test was utilized. Statistical evaluations were performed with Microsoft Excel software. Statistically significant values were defined as $p<0.05$.

Results

All animals survived primary urethral damage and subsequent onlay urethroplasty procedures and were capable of voluntary voiding throughout the study period following 1 week phases of catheterization immediately after each surgical manipulation. At 2 weeks post-electrocoagulation injury, urethroscopic and RUG evaluations demonstrated urethral stricture formation in 92% (N=11/12) of rabbits with a 57±23% mean degree of urethral stenosis relative to uninjured regions in animals presenting strictures (Figure 1A–C). The mean length of urethral strictures observed was 0.81±0.37 cm (N=11). In contrast, no urethral abnormalities were present in these rabbits prior to primary surgical injury (Figure 1B, C). Gross tissue assessments at 1 and 3 months following onlay urethroplasty revealed host tissue ingrowth covering the entire implant site with negligible contraction evident between the proximal/distal or lateral marking sutures (Figure 1A). Longitudinal RUG analyses of repaired urethral segments demonstrated no evidence of contrast extravasation or fistulas across study endpoints (Figure 1B). In addition, the mean degree of urethral stenosis in reconstructed tissues was significantly attenuated by 39% at 3 months post-grafting in comparison to levels observed at 2 weeks following electrocoagulation (Figure 1C). Normal urethral anatomy was also confirmed with urethroscopic evaluations. These data provide evidence that BLSF matrices can restore urethral continuity and mitigating urethral stenosis in injured urethras.

Histological (MTS) evaluations (Figure 2) were performed on damaged and repaired urethral segments to respectively characterize the initial host response to primary injury as well as assess the extent of constructive remodeling at scaffold implantation sites. At 2 weeks post-op, wounded tissues displayed extensive spongiofibrosis obstructing the ventral urethral wall with disruption of smooth muscle bundles and infiltration of mononuclear inflammatory cells evident in the submucosa. These results are consistent with histopathological features commonly observed in patients afflicted with urethral strictures.[18] By 1 month post-repair, cross-sectional organization of de novo urethral tissues revealed a pseudostratified columnar epithelium covering an extracellular matrix (ECM)-rich, vascularized lamina propria. Smooth muscle bundles were concentrated at the periphery of neotissues and fibrotic tissue remodeling was apparent within the interior of the original implant site. Residual fragments of the BLSF matrix were detected in the regenerating tissue and were surrounded by focal areas of putative macrophage phagocytosis. Subepithelial mononuclear inflammatory cells were also found throughout the graft region. Following 3 months post-implantation, 50% of

neotissues exhibited smooth muscle formation within the center of the graft site, however the overall density of smooth muscle bundles was relatively underdeveloped in comparison to the NSC group. In addition, the structure of the neoepithelium at this timepoint was similar to the 1 month timepoint and NSC replicates. Areas of mild fibrosis were still detected in the interior of de novo urethral tissues at this stage of regeneration, while mononuclear inflammatory cells were also localized to the suburothelial compartment. BLSF scaffold fragments were undetectable in the majority of reconstructed urethras.

Reconstructed and control tissues were evaluated by IHC (Figure 3A) and histomorphometric (Figure 3B) analyses to assess the phases of wound healing and determine the degree of maturation achieved over the course of the study. At 2 weeks following primary urethral damage, substantial reductions in α-SMA and SM22α immunoreactivity were detected relative to the NSC group. A similar pattern was observed with NF200+ axon profiles which were evident in NSC, but undetectable at mucosal injury sites. In contrast, pan-CK immunoreactivity was comparable in both the epithelia of NSC and damaged groups. Neotissues at 1 and 3 months following BLSF scaffold implantation contained α-SMA+ and SM22α+ smooth muscle bundles as well as blood vessels. Histomorphometric analyses showed that the degree of α-SMA immunoreactivity in de novo urethral tissues at these timepoints was significantly higher relative to damaged specimens, however these levels only achieved ~30% of NSC. Innervation of neotissues was confirmed at 1 and 3 months postop by the presence of NF200+ axons. In addition, the extent of NF200 immunoreactivity was significantly higher in both these groups in comparison to baseline injury values as well as comparable to NSC levels. Pan-CK+ neoepithelium was found in neotissues at 1 and 3 months following urethral repair with no significant differences detected in respect to NSC and injured groups. These results demonstrate that BLSF grafts promote the formation of innervated, vascularized urethral tissues at sites of previous tissue damage.

Discussion

Tissue engineering strategies for urethral reconstruction have primarily deployed scaffold configurations constructed from decellularized tissues such as SIS or bladder acellular matrix as well as synthetic polyesters including poly-glycolic acid polymers.[19,20] These biomaterials have been investigated as either acellular scaffolds or those seeded with ex vivo expanded, autologous cell sources in predominantly healthy animal models with normal urethras wherein graft anastomosis is performed following primary defect creation.[21–25] Positive regenerative and functional outcomes have been widely reported with the use of these constructs in nondiseased settings of urethral defect consolidation.[19–25] However, these wound microenvironments fail to simulate the fibrotic urethral bed frequently encountered in patients who are in need of urethroplasty such as those with a history of stricture disease, lichen sclerosis, or with prior failed procedures.[26] Therefore, it is not surprising that small-scale, short-term clinical trials of these modalities have reported deleterious side-effects including fibrosis, graft contracture, fistula formation, and incomplete tissue regeneration,[27–30] thus raising doubts about their potential to translate into routine clinical practice.

Protein-based, BLSF matrices possess unique properties for urethral tissue engineering including high structural strength and elasticity, diverse processing flexibility, adjustable biodegradability, and low immunogenicity.[31] In contrast, the physical attributes of ECM-derived scaffolds are dependent upon the characteristics of the source tissue and the mechanical processing methods required for decellularization, hence the options for manipulating the structural, mechanical, and degradative properties necessary to optimize the constructive remodeling response during urethral repair are restricted.[19] In addition, chronic inflammatory reactions elicited by the metabolites of synthetic polyesters have the potential to impede regenerative responses and encourage fibrosis in neotissues.[32,33] Recent reports from our laboratory have demonstrated the ability of acellular BLSF grafts to mediate functional tissue regeneration in various disease models of hollow organ reconstruction including patch esophagoplasty of esophageal strictures[14] as well as augmentation cystoplasty of neurogenic bladders.[34] Therefore, in the current study we investigated the ability of BLSF grafts to facilitate repair of previously damaged urethral tissues in a rabbit model of onlay urethroplasty.

Prior to scaffold implantation, primary urethral damage was induced by electrocoagulation to generate a focal, partial thickness defect. This approach was utilized to encourage scar tissue formation while minimizing the risk of fistula formation from a full thickness injury. By 2 weeks postop, spontaneous wound healing of the urethral wall was limited with significant reductions in smooth muscle and innervation markers observed in comparison to NSC. In contrast, re-epithelialization of the original defect region had occurred at this timepoint presumably to restore the blood-urine barrier and prevent further urinary extravasation. Consistent with previously published observations,[16] stricture formation was present in the majority of study replicates 2 weeks following injury due to putative fibroproliferative tissue remodeling.

Reconstruction of diseased urethras with BLSF grafts demonstrated that these biomaterials can promote constructive remodeling as well as mitigation of urethral stenosis in an environment of tissue damage and fibrosis. Similar to our past study in a nondiseased urethroplasty model,[11] BLSF matrices supported the formation of innervated, vascularized neotissues at defect sites without significant induction of chronic inflammatory reactions characterized by mobilized follicular aggregates of mononuclear cell infiltrates frequently observed with SIS matrix implantation. However, BLSF grafts failed to achieve complete smooth muscle regeneration relative to NSC as was seen during primary urethral defect repair[11] suggesting that prior urethral damage attenuates this aspect of the wound healing process following reconstruction. These findings are consistent with the results of Villoldo and colleagues wherein smooth muscle formation at SIS graft sites was attenuated in diseased urethras.[13]

The limitations of the present study include the small cohort of rabbits used for each experimental group and the relatively short-term implantation periods. In addition, functional assessments of reconstructed tissues such as uroflowmetry as well as penile curvature measurements to demonstrate adequate elasticity to sustain a penile erection are needed in future investigations before consideration of clinical translation. Furthermore, validation of the ability of BLSF grafts to repair strictures >2 cm in length is necessary since

primary anastomotic urethroplasty is generally performed with high success rates for stricture lengths described in this report.[35] Finally, performance assessments of our scaffold technology in a female model of urethral repair are required to identify any gender-specific differences in wound healing potential. Nevertheless, our data suggest that BLSF matrices may be a valuable clinical option for replacement of diseased urethral tissues.

In conclusion, our results demonstrate the potential of BLSF matrices to reconstruct chronically damaged urethras in a rabbit model of onlay urethroplasty. These scaffolds facilitate de novo tissue formation at graft sites and attenuate urethral stenosis following primary injury. Future preclinical evaluations will focus on interrogating the capacity of BLSF scaffolds to repair long urethral strictures while preserving voiding and sexual function. In addition, direct comparisons of BLSF grafts with standard of care, autologous tissue grafts in preclinical models of urethral reconstruction will be pursued.

Acknowledgments

This research was supported by NIH/NIBIB 1R21EB021482-01 (J.R.M and C.R.E.). The authors thank Drs. Frank-Mattias Schäfer and Gokhan Gundogdu for technical assistance and helpful discussions and acknowledge the Tufts University, Tissue Engineering Resource Center, NIH/NIBIB P41 EB002520 (KAPLAN), for procurement of silkworm cocoons.

References

1. Keays MA, Dave S. Current hypospadias management: Diagnosis, surgical management, and long-term patient-centred outcomes. Can Urol Assoc J. 2017; 11:S48–S53. [PubMed: 28265319]
2. Bayne DB, Gaither TW, Awad MA, Murphy GP, Osterberg EC, Breyer BN. Guidelines of guidelines: a review of urethral stricture evaluation, management, and follow-up. Transl Androl Urol. 2017; 6:288–294. [PubMed: 28540238]
3. Horiguchi A. Substitution urethroplasty using oral mucosa graft for male anterior urethral stricture disease: Current topics and reviews. Int J Urol. 2017; 24:493–503. [PubMed: 28600871]
4. Levy ME, Elliott SP. Graft Use in Bulbar Urethroplasty. Urol Clin North Am. 2017; 44:39–47. [PubMed: 27908370]
5. Sugita Y, Tanikaze S, Yoshino K, Yamamichi F. Severe hypospadias repair with meatal based paracoronal skin flap:the modified Koyanagi repair. J Urol. 2001; 166:1051–1053. [PubMed: 11490297]
6. Snodgrass WT. Snodgrass technique for hypospadias repair. BJU Int. 2005; 95:683–693. [PubMed: 15705110]
7. Baskin LS, Ebbers MB. Hypospadias: anatomy, etiology, and technique. J Pediatr Surg. 2006; 41:463–472. [PubMed: 16516617]
8. Scuderi N, Chiummariello S, De Gado F. Correction of hypospadias with a vertical preputial island flap: a 23-year experience. J Urol. 2006; 175:1083–1087. [PubMed: 16469625]
9. Kumar A, Das SK, Trivedi S, Dwivedi US, Singh PB. Substitution urethroplasty for anterior urethral strictures: buccal versus lingual mucosal graft. Urol Int. 2010; 84:78–83. [PubMed: 20173374]
10. Seth A, Chung YG, Gil ES, Tu D, Franck D, Di Vizio D, Adam RM, Kaplan DL, Estrada CR Jr, Mauney JR. The performance of silk scaffolds in a rat model of augmentation cystoplasty. Biomaterials. 2013; 34:4758–4765. [PubMed: 23545287]
11. Chung YG, Tu D, Franck D, Gil ES, Algarrahi K, Adam RM, Kaplan DL, Estrada CR Jr, Mauney JR. Acellular bi-layer silk fibroin scaffolds support tissue regeneration in a rabbit model of onlay urethroplasty. PLoS One. 2014; 9:e91592. [PubMed: 24632740]
12. Akbal C, Lee SD, Packer SC, Davis MM, Rink RC, Kaefer M. Bladder augmentation with acellular dermal biomatrix in a diseased animal model. J Urol. 2006; 176:1706–1711. [PubMed: 16945628]

13. Villoldo GM, Loresi M, Giudice C, Damia O, Moldes JM, DeBadiola F, Barbich M, Argibay P. Histologic changes after urethroplasty using small intestinal submucosa unseeded with cells in rabbits with injured urethra. Urology. 2013; 81:e1–5. [PubMed: 23273096]
14. Algarrahi K, Franck D, Savarino A, Cristofaro V, Yang X, Affas S, Schäfer FM, Sullivan MP, Estrada CR Jr, Mauney JR. Bilayer silk fibroin grafts support functional oesophageal repair in a rodent model of caustic injury. J Tissue Eng Regen Med. 2018; 12:e1068–e1075. [PubMed: 28371514]
15. Blaschko SD, Breyer BN, McAninch JW. Reoperative urethroplasty. A systematic review. Arch Esp Urol. 2014; 67:138–141. [PubMed: 24531682]
16. Faydaci G, Tarhan F, Tuncer M, Eryildirim B, Celik O, Keser SH, Ozgül A. Comparison of two experimental models for urethral stricture in the anterior urethra of the male rabbit. Urology. 2012; 80:225e7–11.
17. Andersen HL, Duch BU, Nielsen JB, Joergensen B, Ledet T. An experimental model for stricture studies in the anterior urethra of the male rabbit. Urol Res. 2003; 31:363–367. [PubMed: 14520504]
18. Tritschler S, Roosen A, Füllhase C, Stief CG, Rübben H. Urethral stricture: etiology, investigation and treatments. Dtsch Arztebl Int. 2013; 110:220–226. [PubMed: 23596502]
19. Ribeiro-Filho LA, Sievert KD. Acellular matrix in urethral reconstruction. Adv Drug Deliv Rev. 2015; 82–83:38–46.
20. Atala A, Danilevskiy M, Lyundup A, Glybochko P, Butnaru D, Vinarov A, Yoo JJ. The potential role of tissue-engineered urethral substitution: clinical and preclinical studies. J Tissue Eng Regen Med. 2017; 11:3–19. [PubMed: 26631921]
21. Kropp BP, Ludlow JK, Spicer D, Rippy MK, Badylak SF, Adams MC, Keating MA, Rink RC, Birhle R, Thor KB. Rabbit urethral regeneration using small intestinal submucosa onlay grafts. Urology. 1998; 52:138–142. [PubMed: 9671888]
22. Chen F, Yoo JJ, Atala A. Acellular collagen matrix as a possible “off the shelf” biomaterial for urethral repair. Urology. 1999; 54:407–410. [PubMed: 10475343]
23. De Filippo RE, Yoo JJ, Atala A. Urethral replacement using cell seeded tubularized collagen matrices. J Urol. 2002; 168:1789–1792. [PubMed: 12352360]
24. Huang X, Luo J, Liao Y, Qu Y, Yang Z. Study on small intestinal submucosa as repair materials in urethral reconstruction. Zhongguo Xiu Fu Chong Jian Wai Ke Za Zhi. 2006; 20:206–209. [PubMed: 16579221]
25. Li C, Xu YM, Song LJ, Fu Q, Cui L, Yin S. Urethral reconstruction using oral keratinocyte seeded bladder acellular matrix grafts. J Urol. 2008; 180:1538–1542. [PubMed: 18710759]
26. Versteegden LRM, de Jonge PKJD, IntHout J, van Kuppevelt TH, Oosterwijk E, Feitz WFJ, de Vries RBM, Daamen WF. Tissue Engineering of the Urethra: A Systematic Review and Meta-analysis of Preclinical and Clinical Studies. Eur Urol. 2017; 72:594–606. [PubMed: 28385451]
27. Atala A, Guzman L, Retik AB. A novel inert collagen matrix for hypospadias repair. J Urol. 1999; 162:1148–1151. [PubMed: 10458452]
28. Palminteri E, Berdondini E, Colombo F, Austoni E. Small intestinal submucosa (SIS) graft urethroplasty: short-term results. Eur Urol. 2007; 51:1695–1701. [PubMed: 17207913]
29. Fiala R, Vidlar A, Vrtal R, Belej K, Student V. Porcine small intestinal submucosa graft for repair of anterior urethral strictures. Eur Urol. 2007; 51:1702–1708. [PubMed: 17306922]
30. Farahat YA, Elbahnasy AM, El-Gamal OM, Ramadan AR, El-Abd SA, Taha MR. Endoscopic urethroplasty using small intestinal submucosal patch in cases of recurrent urethral stricture: a preliminary study. J Endourol. 2009; 23:2001–2005. [PubMed: 19839728]
31. Sack BS, Mauney JR, Estrada CR Jr. Silk Fibroin Scaffolds for Urologic Tissue Engineering. Curr Urol Rep. 2016; 17:16. [PubMed: 26801192]
32. Ceonzo K, Gaynor A, Shaffer L, Kojima K, Vacanti CA, Stahl GL. Polyglycolic acid-induced inflammation: role of hydrolysis and resulting complement activation. Tissue Eng. 2006; 12:301–308. [PubMed: 16548688]
33. Mauney JR, Cannon GM, Lovett ML, Gong EM, Di Vizio D, Gomez P 3rd, Kaplan DL, Adam RM, Estrada CR Jr. Evaluation of gel spun silk-based biomaterials in a murine model of bladder augmentation. Biomaterials. 2011; 32:808–818. [PubMed: 20951426]

34. Chung YG, Algarrahi K, Franck D, Tu DD, Adam RM, Kaplan DL, Estrada CR Jr, Mauney JR. The use of bi-layer silk fibroin scaffolds and small intestinal submucosa matrices to support bladder tissue regeneration in a rat model of spinal cord injury. Biomaterials. 2014; 35:7452–7459. [PubMed: 24917031]

35. Jordan, GH., McCammon, KA. Surgery of the Penis and Urethra. Vol. 1. Oxford: Elsevier Saunders; 2012. p. 956-1000.

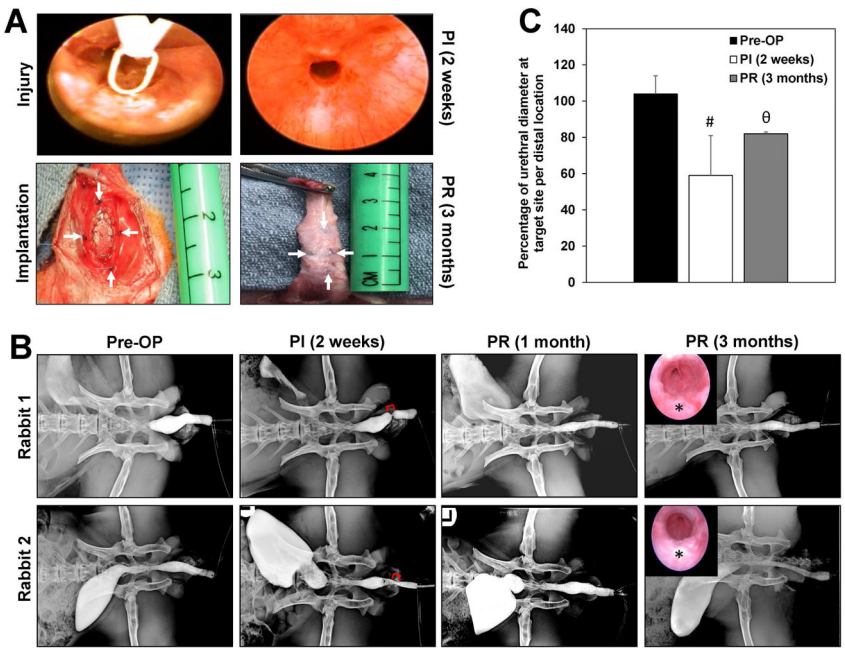

Figure 1. Surgical urethral procedures and imaging evaluations of injury and repair responses

[**A**] Top row: Urethroscopic evaluation of the electrocoagulation injury site during creation (left panel) and 2 weeks post-injury (PI) (right panel). Bottom row: Vetral onlay urethroplasty model with BLSF graft (left panel) and de novo tissue formation 3 months post-repair (PR). Arrows denote marking sutures. [**B**] Longitudinal RUG analyses of two representative animals at pre-op, 2 weeks following primary urethral damage, and over the course of 3 months after BLSF scaffold implantation. Brackets denote urethral strictures. Insets: Urethroscopic images of repaired urethras at 3 months post-op. (*) denotes original graft region. [**C**] Quantitation of the degree of urethral stenosis calculated from RUG analyses. Means ± standard deviation. (#) = $p<0.05$ in comparison to NSC. (θ) = $p<0.05$ in comparison PI (2 weeks). Data in panel C was acquired from N=5 animals across longitudinal timepoints.

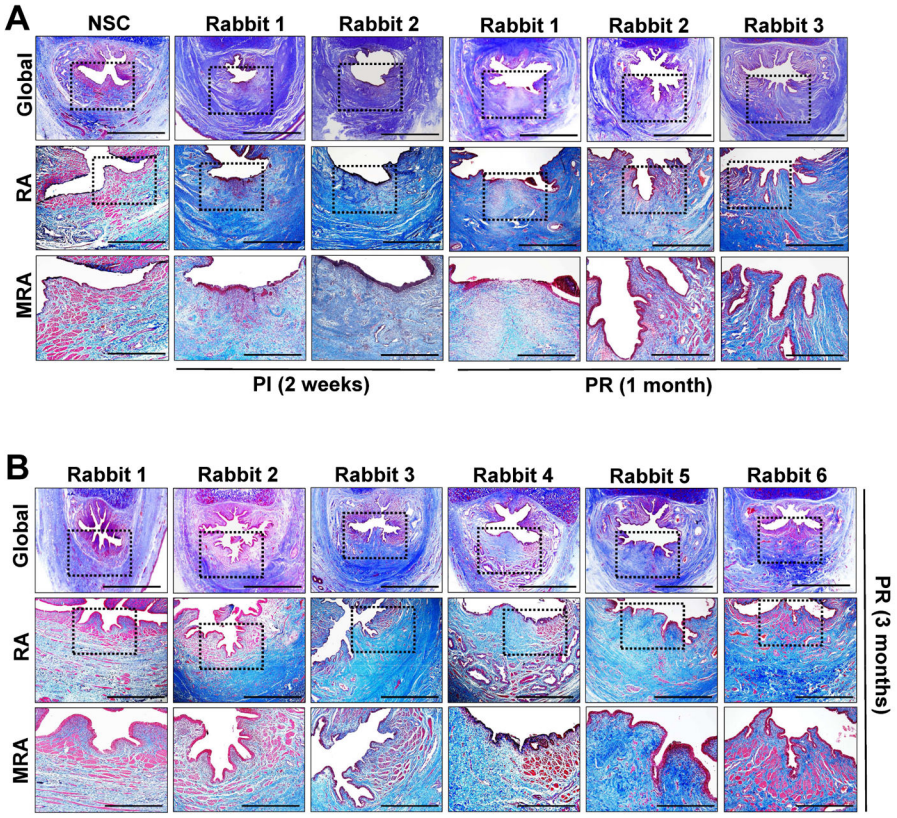

Figure 2. Histological analyses of primary urethral damage and constructive remodeling following urethroplasty

[**A–B**] 1st rows: Photomicrographs of MTS-stained, gross urethral cross-sections from NSC and penile segments containing the original electrocoagulation site 2 weeks post-injury (PI) as well as de novo tissues at 1 and 3 months post-repair (PR) with BLSF grafts. Boxed areas encompass baseline NSC architecture or surgically manipulated areas in experimental groups. Scale bars = 3 mm. 2nd rows: Magnification of global tissue regeneration area (RA) in damaged and repaired groups as well as controls boxed in top rows. Scale bars = 1.5 mm. 3rd rows: Magnified boxed areas in 2nd rows displaying mucosal regions in control and experimental cohorts. Scale bars = 600 μm.

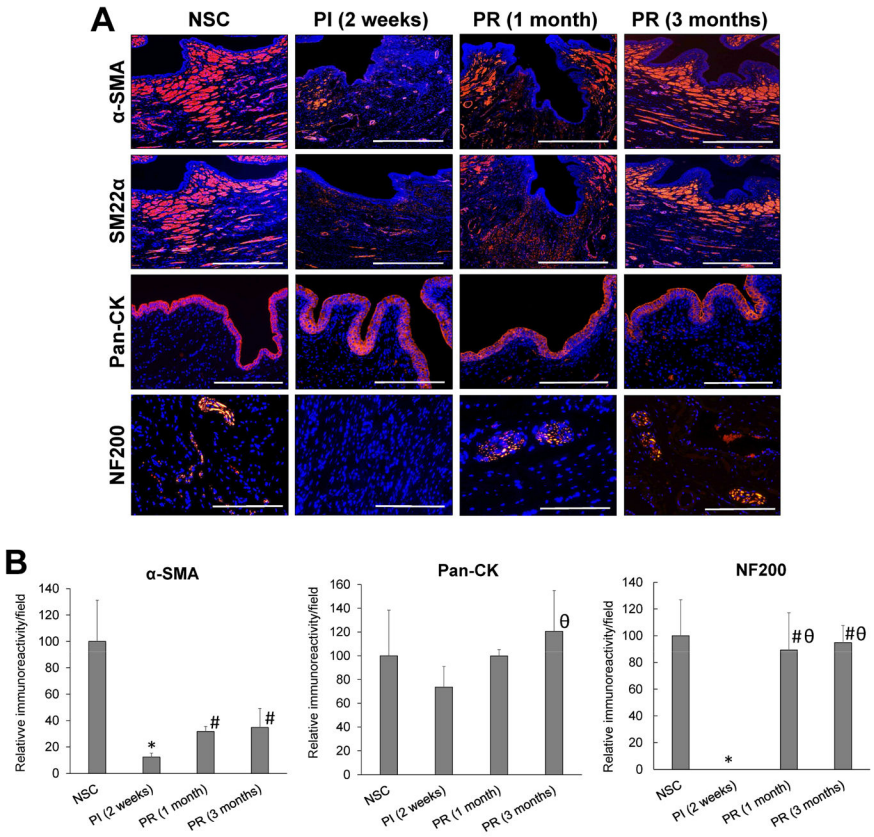

Figure 3. IHC and histomorphometric assessments of urethral injury and repair responses following BLSF scaffold implantation

[**A**] Photomicrographs of α-SMA, SM22α, pan-CK, and NF200 protein expression in urethral mucosa from NSC, original electrocoagulation site 2 weeks post-injury (PI), and regenerated tissues at 1 and 3 months post-repair (PR) with BLSF scaffolds. For all panels, respective marker expression is displayed in red (Cy3 labeling) and blue denotes DAPI nuclear counterstain. Scale bars for α-SMA and SM22α panels = 200 μm and for pan-CK and NF200 panels = 800 μm. [**B**] Histomorphometric analysis of stained elements displayed in [A]. Means ± standard deviation. (*) = $p<0.05$ in comparison to NSC. (#) = $p<0.05$ in comparison PI (2 weeks). (θ) = $p>0.05$ in comparison to NSC. Data in all panels was acquired from N=3–5 animals per experimental group.